ISBN: 978-3-95450-262-2 ISSN: 2673-5350 doi: 10.18429/JACoW-IBIC2025-MOCI01

COMMISSIONING AND FIRST OPERATION OF SLS 2.0, THE UPGRADE OF THE SWISS LIGHT SOURCE

B. Keil on behalf of the SLS 2.0 Team
PSI Center for Accelerator Science and Engineering, Villigen, Switzerland

Abstract

After more than 20 years of successful operation, the storage ring of the Swiss Light Source (SLS) has recently been replaced with a new diffraction-limited storage ring (DLSR) called SLS 2.0. After a dark time of 15 months from October 2023 until December 2024, SLS 2.0 now provides more than 40 times higher brilliance for hard X-ray users, thanks to an innovative compact 7-bend achromat magnet lattice with reverse bending magnets that fits into the old SLS 1.0 tunnel. In this contribution, we give an overview of the commissioning of the new storage ring and first user operation experience, highlighting key differences between SLS 1.0 and 2.0, as well as the role and usage of different beam instrumentation systems during the commissioning process from the operations perspective. Moreover, we present the status of beam-based feedback systems, and the resulting beam stability and performance that has been achieve so far during first user operation.

INTRODUCTION

Table 1 provides an overview of the key parameters of the SLS 1.0 and SLS 2.0 storage ring [1]. In addition to a more than 40 times higher brilliance, SLS 2.0 also has an increased electron energy of 2.7 GeV. Combined with newly designed insertion devices, SLS 2.0 provides a 50 % higher hard X-ray photon energy range.

Table 1: SLS Storage Ring Beam Parameters

Parameter	Units	SLS 1.0	SLS 2.0
Circumference	m	288	
Beam Current	mA	400	
Injection Charge	nC	~0.01-0.4 @ 3 Hz	
Beam Energy	GeV	2.4	2.7
Main RF	MHz	499.637	499.654
Harmonic No.	#	480	
Hor. Emittance	pm	5030	131-158
Vert. Emittance	pm	5-10	10
Hor. Tune		20.43	39.37
Vert. Tune		8.74	15.22
Ring BPMs	#	75	136

While the SLS storage ring and most of its subsystems required a completely new design to achieve the requested design parameters of the SLS 2.0 project, the original SLS 1.0 linac and full energy booster synchrotron could be re-used, thanks to the low booster emittance of 12 pm.rad that is sufficient for high SLS 2.0 injection efficiency. The few upgrades of linac and booster that were performed during the SLS dark time include a new gun pulser, as well as a replacement of the ageing 1000 A power supply of the combined function booster main dipole magnets. Linac and booster are currently still using the original SLS 1.0 BPM system and magnet power supplies (except for the main dipole circuit). Although these systems meet SLS 2.0 requirements, they are scheduled to be upgraded 2026+ for maintenance reasons, where the BPM and magnet cables have already been replaced.

INJECTOR RECOMMISSIONING

In order to save time for the storage ring commissioning scheduled for mid-January 2025, the linac was recommissioned already in November 2024, and the booster in December 2024, while the storage ring and its subsystems were still being installed. Both linac and booster reached their design performance within less than one week, including the extraction of the 2.7 GeV booster beam through the newly designed booster-to-ring transfer line up to the storage ring septum [2].

STORAGE RING COMMISSIONING

Getting the First Turn

On January 14, 2025, the beam commissioning of the new SLS 2.0 storage ring started [3, 4], following careful pre-beam tests of all systems and components. After optics matching of injected beam to stored beam via screen monitors, the first turn in the ring was achieved using only two dipole corrector magnets after the septum, while tuning septum and injection kickers, as well as booster / transfer line energy and trajectory using RF BPMs (see Fig. 1).

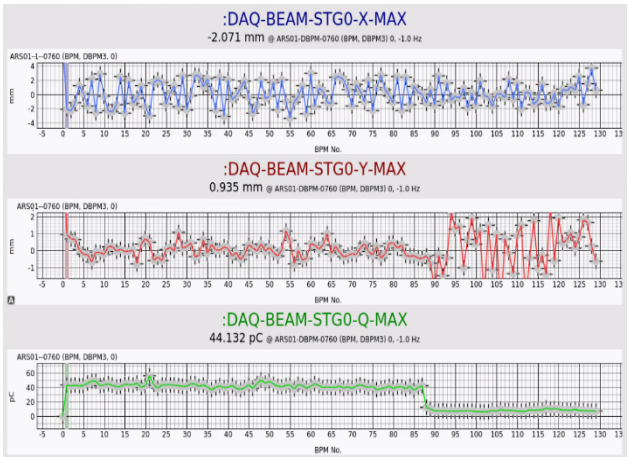

Figure 1: Storage ring horizontal orbit (top, blue), vertical orbit (middle, red), and bunch charge (bottom, green), measured by BPMs in turn-by-turn mode. The beam was intentionally blocked at BPM no. 87 by a closed valve.

ISBN: 978-3-95450-262-2 ISSN: 2673-5350 doi: 10.18429/JACoW-IBIC2025-MOCI01

In contrast to the SLS 1.0 ring that had only electromagnets (except for undulators), the permanent dipole magnets of the SLS 2.0 ring result in a fixed ring beam energy. Thus, we had to vary the energy of the injected beam by changing booster current ramps and transfer lines magnet settings to match booster and ring energy and thus optimize the booster-to-ring charge transfer efficiency.

BPMs: Optimizing the Ring Beam Trajectory

At SLS 2.0 startup, the digital downconverters (DDCs) of the newly developed ring RF BPM system [5] were configured to provide three data streams simultaneously: 4 MSamples/s turn-by-turn (TBT) data, 20 kSamples/s for the fast orbit feedback data, and 20 Samples/s for slow orbit correction and graphical user interfaces (GUI). The TBT data provided a clean separation of charge and position readings for every turn even without tuning trigger delays or synchronizing the DDCs.

Additional noise suppression of TBT data was supported by a feature of the BPM firmware called "ADC peak filtering" that detects beam signals in the ADC data using a configurable threshold and sample window size around the beam signals. ADC noise outside this window is cancelled by zeroing the samples before they enter the first stage of the digital downconverter (DDC) of the BPM system, thus reducing the TBT data noise when filling just a fraction of the 480 ring RF buckets with charge.

While trying to get several turns, the BPM charge (button sum signal) readings showed unexpected beam loss upstream of the passive 3rd harmonic cavity (3HC) of the storage ring, as did the dedicated beam loss monitors [6]. After detecting and realigning a misaligned beam pipe taper at this location, these abnormal losses disappeared. Iterative orbit, energy and magnet optics optimization with turn-by-turn BPM data then lead to a growing number of turns. After switching on the 500 MHz high power RF system of the storage ring consisting of four new HOM-damped cavities with new solid state power amplifiers, BPM readings at dispersive BPMs were used to tune the RF cavity phase until the amplitude of the synchrotron oscillation visible at the dispersive BPM was minimized, confirming that the RF phase was correct and just compensated the radiation loss of the injected beam that is 668 keV for SLS 2.0.

Stored Beam and Accumulation

On January 23, nine days after the first injection attempt, stored beam was achieved, and soon also accumulation. The betatron tune was measured and corrected using BPM turn-by-turn data and dedicated tune pinger magnets. With stored beam, the DDC stage 2 (20 Samples/s) high-resolution BPM data simplified orbit and optics correction.

Booster-to-Ring Charge Transfer Efficiency

The booster-to-ring charge transfer efficiency was initially limited to about 40 % (for the fraction of the booster charge that could be injected and stored/accumulated in the ring), where both BPMs and beam loss monitors (BLMs) showed unexpected charge loss directly after the injection septum. The reason was found to be a misaligned valve. After fixing the valve position, up to 97 % booster-to-ring charge transfer efficiency has been achieved.

Reaching 400 mA Design Current

After successful accumulation in January, we had a self-imposed beam current of 25 mA until mid of March, since the newly designed beam dump kicker system, triggered by the machine protection system (MPS) [7], was not yet ready, but required to protect the machine from uncontrolled beam losses at high beam current. On March 11, the beam dump kicker system was completed and successfully tested, where the TBT readings of the BPMs confirmed that the kicker dumped nearly the full beam charge within an single turn as required (see Fig. 2), using a dedicated copper target to absorb the beam power safely.

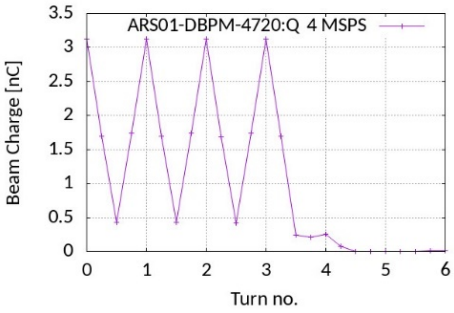

Figure 2: Beam charge measured with a BPM turn-by-turn, during successful test of the new beam dump kicker.

After the successful kicker tests, we gradually increased the beam current, limited by the safety thresholds of the vacuum systems. An automated injection system kept the beam current below the vacuum interlock threshold. During the increase of the beam current, newly developed coupled bunch mode (CBM) instability detection systems with very high sensitivity were operational transversely and longitudinally [8]. The detection threshold is about 100x lower than the level where a CBM instability may become dangerous for the accelerator. On April 6, we reached the design current of 400 mA for several hours. As predicted by previous simulations, no longitudinal or transverse CBM instabilities occurred. Initially, some ion instabilities were observed also via BPMs and beam size monitors, but they could be successfully suppressed using one (or temporarily two) gaps of 30-50 buckets in the bunch train.

FILLING PATTERN MEASUREMENT AND FEEDBACK

From day one of SLS 1.0 commissioning, a BPM-based filling pattern (FP) measurement was available, where the sum signal of a BPM was digitized by an RF System-on-Chip (RFSoC). The RFSoC combines eight 4 GSamples/s 12-bit ADCs, eight 6.5 GSamples/s DACs, a large FPGA, two performant multi-core CPUs as well as multi-gigabit links on a single chip [8]. On one CPU, we have implemented a filling pattern feedback (FPFB) that has been successfully commissioned recently. Before, a feed-forward control was used to fill the RF buckets in a pre-defined order periodically. The FPFB automatically injects the beam

ISBN: 978-3-95450-262-2 ISSN: 2673-5350 doi: 10.18429/JACoW-IBIC2025-MOCI01

into suitable buckets, using a real-time gigabit fiber link to the event system master, such that a user-defined filling pattern and beam current is obtained [8]. The RFSoC of the system also dumps the beam via a trigger to the MPS if the charge in a bunch exceeds a user-defined threshold, thus protecting the accelerator from excessive single-bunch charge that may damage components like the 3HC.

The RFSoC based FPFB also receives data via a gigabit fiber link from a complementary FP measurement system that uses a photodiode exposed to synchrotron radiation [6]. This system became available several weeks after the BPM based system. Its resolution is currently significantly lower than the BPM based FP measurement, but it is still sufficient and valuable in case one of the system fails.

MULTIBUCH DIAGNOSTICS AND FEEDBACK

The BPM based FP measurement not only provides the charge of each single bunch, but also the bunch arrival time of each bunch, by oversampling the sum signal of an RF BPM with 64 GSamples/s, by using a 4 GSamples/s ADC of the RFSoC with a fractional clock providing interleaved samples over 16 turns. On this arrival time data, longitudinal CBM instabilities would be visible as spatial modulation of the arrival time of the individual bunches. Thus, we use it as longitudinal CBM instability detector, providing a sensitivity of ~100 fs at 400 mA (with 450 of 480 RF buckets filled). This resolution is far below the level of ~60 ps where a CBM might become dangerous for the RF system.

Detection of transverse CBM instabilities has also been implemented using an RFSoC, where an ADC does interleaved sampling of the difference signal of BPM button electrodes that is proportional to the product of beam position and charge of each bunch. With a 4 GSamples/s ADC and 16 times interleaved oversampling, the RFSoC detects CBM instabilities that would be visible as spatial amplitude modulation of the signal along the bunch train.

Both transverse and longitudinal CBM detectors provide the mode spectrum, as well as an integral sum of all mode amplitudes as a single number, where an unexpected increase of this number raises an alarm, with the option to dump the beam if a user-define threshold is exceeded.

Transverse Multibunch Feedback

Although SLS 2.0 was not expected to have CBM instabilities, and none were observed so far, we took an RFSoC based transverse multibunch feedback developed at PSI into operation, and successfully demonstrated its operation by damping the beam after excitation with a pinger magnet [8]. Features like tune measurement, excitation/damping scans etc. are under development. So far, the transverse MBFB uses the commercial SLS 1.0 MBFB RF front-end electronics (RFFE) that mixes a 1.5 GHz button BPM sum/difference signal to baseband, where the RFSoC then samples and processes the baseband signal. A direct sampling RFFE without mixer and a suitable modification of the MBFB algorithm (implemented in VHDL on the RFSoC) is under development.

Longitudinal Multibunch Feedback

A longitudinal MBFB using the SLS 1.0 RFFE has been nearly completed, where we would only need to modify the analog SLS 1.0 upconverter for the kicker power amplifier to make it operational, since the SLS 1.0 kicker operated at 1.375 GHz, while the SLS 2.0 kicker has 1.875 GHz. However, since the system is not required to reach 400 mA, we decided to skip this final step as long as there is no urgent need for the system. Instead, we intend to drive the kicker power amplifier directly, by synthesizing a suitable waveform with the fast DACs of the RFSoC. We have already demonstrated that this is possible, by driving the complete kicker system from the RFSoC and measuring the kicker response with a test pickup in the kicker [9]. The integration of this scheme into the MBFB engine is planned.

ORBIT FEEDBACK COMPONENTS

Dipole Corrector Magnets and Power Supplies

The SLS 2.0 ring uses 115 BPMs and 115 dipole corrector magnets per plane (horizontal and vertical) for its orbit feedback. There is only one type of corrector magnet that is both fast and strong, having iron yokes with 0.35 mm lamination thickness, and a 0.5 mm thick stainless steel beam pipe, while the normal SLS 2.0 beam pipe is made of NEG-coated copper. The low-noise corrector magnet power supplies were developed at PSI, like all other SLS 2.0 magnet power supplies. The vertical correctors have ±400 µrad kick angle, the horizontal ones ±600 µrad thanks to extra coils on the yokes providing more kick angle for static corrections during first beam commissioning, at the expense of a slightly lower bandwidth. After beam-based component realignment that is still ongoing, it is planned to bypass the extra coils, thus providing ±400 µrad kick angle and equal corrector bandwidth in both planes.

The complete system of corrector power supply, magnets and 0.5 mm stainless steel beam pipe presently has a small signal -3 dB bandwidth of ~3 kHz, measured with beam by exciting the corrector at different frequencies and measuring the beam response with a suitable wideband BPM DDC filter. An increase of the corrector bandwidth is planned by replacing the present PID controller algorithm of the power supply firmware with an advanced version that applies additional predictive feed-forward control of the PS MOSFET duty cycle for a faster corrector response.

BPMs

As already mentioned, the ring BPM firmware supports three different data streams, where the sample rate and bandwidth of each stream can be freely programmed during operation using a Python GUI. Initially, we used 4 MSamples/s for the TBT data stream, 20 kSamples/s for the fast orbit feedback (FOFB) data stream, and 20 Samples/s for the slow data stream intended for slow orbit correction, analysis and GUI orbit displays. Lately, we use 2 MSamples/s, 74 kSamples/s, and 20 Samples/s, to have longer TBT waveforms and lower FOFB loop latency.

ISBN: 978-3-95450-262-2 ISSN: 2673-5350 doi: 10.18429/JACoW-IBIC2025-MOCI01

Slow and Fast Orbit Feedback Engine

In the first months of commissioning, we used only a slow orbit feedback (SOFB) with ~0.5 Hz correction rate that was sufficient for accelerator commissioning. An initial SOFB version was implemented in a Python program running on a PC, reading the BPM data and setting the corrector magnet currents via EPICS. In a 2nd step, we implemented the feedback algorithm in programmable logic (VHDL) on a Zynq Ultrascale+ MPSoC, receiving the BPM data also via EPICS, but setting the corrector magnet currents already via fast fiber optic links.

In June 2025, shortly before the first user pilot experiments, we successfully implemented the third and final step, where we receive the BPM data also via fast multi-gigabit fiber links, using an in-house protocol. The FOFB engine running on the Zynq UltraScale+ is not connected to the BPM electronics directly, but via 12 switches (one per sector of the ring), where each switch is connected to 4 DBPM3 units that provide data of up to 3 BPMs each. The switches also provide connectivity to the corrector magnet power supplies, thus the single central FOFB engine receives BPM data and sets corrector data using the same 12 switches that use AMD Artix-7 and Kintex-7 FPGAs for the interfaces to BPMs, correctors, and central feedback engine, with a custom fiber link protocol developed at PSI.

FOFB ALGORITHM

While SLS 1.0 used an optics model to determine the corrector-BPM response matrix for the FOFB, SLS 2.0 FOFB uses a measured beam response matrix to calculate the corrector set values from the BPM readings, using SVD inversion with Tikhonov regularization. Initially, we had planned to use separate matrices for horizontal (X) and vertical (Y) plane. However, the feedback engine was already designed to use a fully coupled X/Y correction matrix, and after we measured and SVD-inverted one, we found it is working well, and now use a fully coupled X/Y correction.

The FOFB algorithm first calculates the ideal set value for each corrector that would be needed for a 100 % correction of the measured orbit error, and then feeds it into one PID controller per power magnet PS can be individually tuned, e.g. to manage small differences in the bandwidth between different corrector magnets.

Dispersion and RF Frequency Correction

Normally, the FOFB should not correct energy oscillations of the beam (e.g. mode-0 instabilities) or intentional changes of the RF frequency and orbit circumference resulting in horizontal orbit variations that are proportional to the dispersion function at the BPMs. Therefore, the FOFB projects the measured orbit error (difference between measured and desired orbit) onto a measured dispersion unity vector, and then subtracts the dispersive part of the error from the orbit error. With the resulting orbit error vector, it performs a normal SVD-based correction.

However, by making the dispersion unity vector slightly smaller than one (where we can adjust the length), we make the FOFB correct dispersion orbits very slowly, rather than not at all. We also tune the RF frequency constantly, such that the resulting average orbit has a user-defined value for the weighted integral of all horizontal corrector kicks. This scheme makes sure that this integral and thus the beam energy remains constant, while the RF frequency is usually not constant, e.g. when the storage ring warms up and expands after a longer shutdown.

For this scheme, we determine the weights for the corrector kick integral by measuring the corrector response that is needed to generate a dispersion orbit. After normalizing the length of this vector to 1, we calculate its scalar product with the horizontal corrector current vector to obtain the weighted horizontal corrector current.

ORBIT STABILITY AND BPM NOISE

When we first had stored beam, we found it had an orbit perturbation of ~10 µm peak-peak in both planes when the booster was ramping with 3.125 Hz. During top-up operation at 400 mA, the booster performs several injections every few minutes, usually with 4 mA hysteresis of the top-up current. Thus, without orbit feedback, the booster generates an orbit perturbation every few minutes in the order of the beam size, making the FOFB mandatory for user operation to suppress this perturbation. Without ramping booster, we observed orbit perturbations in the ring mainly with several 100 nm amplitude at 50 Hz and 90 Hz, where the latter are a known eigenfrequency of the BPM girders that was measured before first beam with an accelerometer.

Figure 3 shows the dominant horizontal orbit perturbation modes and their RMS amplitudes with fast orbit feedback switched off (top) and on (bottom) running with 40 kHz correction rate. Figure 4 shows the corresponding vertical perturbations. The overall orbit RMS motion is reduced by the FOFB from 564 nm to 144 nm horizontally (factor 4) and from 648 nm to 91 nm vertically (factor 7). Since these RMS values include BPM electronics noise of typically 30-40 nm RMS, the real improvement is even larger. The data was taken from all BPMs (in-loop and out-of-loop).

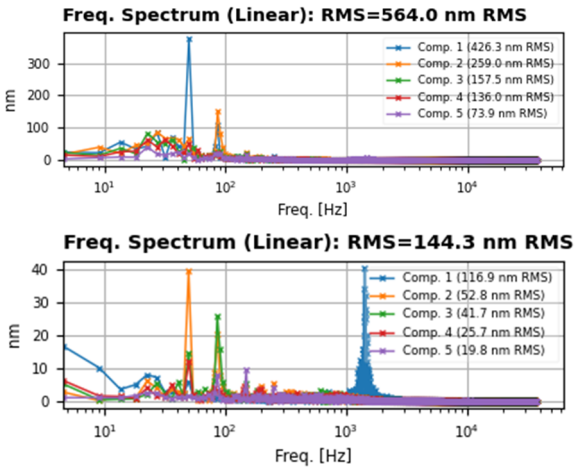

Figure 3: Horizontal orbit motion spectrum (dominant eigenmodes) with FOFB and booster switched off (top) and with both switched on (bottom).

ISBN: 978-3-95450-262-2 ISSN: 2673-5350 doi: 10.18429/JACoW-IBIC2025-MOCI01

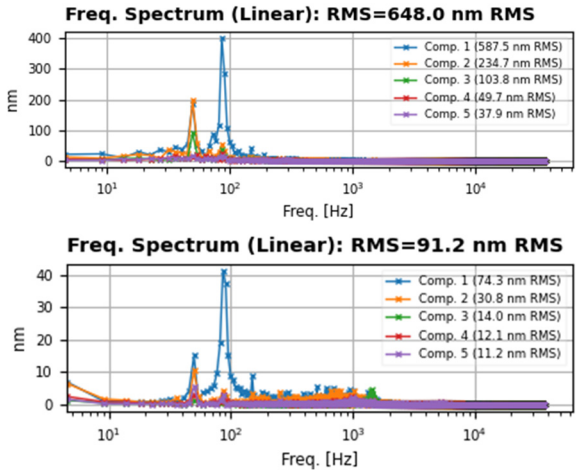

Figure 4: Vertical orbit motion (dominant eigenmodes) with FOFB and booster off (top) and on (bottom).

Figure 5 shows the beam position frequency spectrum of the FOFB data stream at 400 mA for an out-of-FOFB-loop BPM (~3 kHz -3 dB bandwidth), including both BPM noise and real orbit perturbations. Figure 6 shows a spectrum, where the position was calculated from the internal RFFE pilot tone +2.551 MHz above the 499.654 MHz beam signal. This spectrum contains only electronics noise. The BPM ADCs were at ~60 % full scale (~40 % for the beam and ~20 % for the pilot signal), resulting in a position noise of the BPM electronics of 30 nm RMS from 1 Hz to 3 kHz.

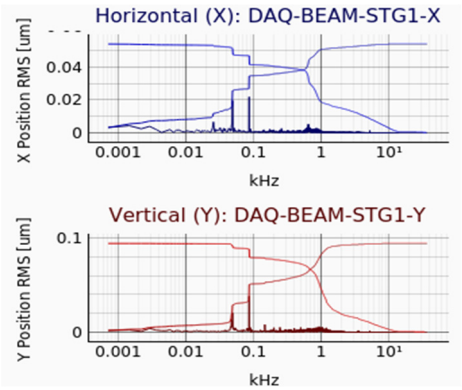

Figure 5: Spectrum of BPM electronics beam signal X/Y position readings (3 kHz DDC bandwidth, 400 mA beam).

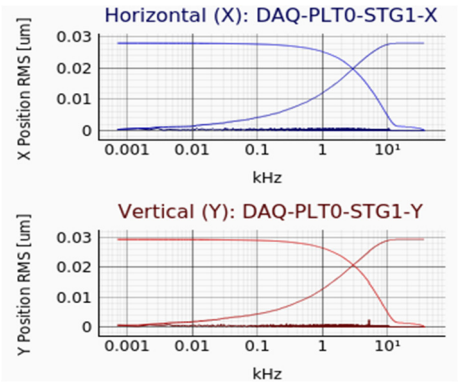

Figure 6: Spectrum of BPM electronics pilot signal X/Y position readings (3 kHz DDC bandwidth, 400 mA beam).

SUMMARY AND OUTLOOK

SLS 2.0 has been successfully commissioned, utilizing a carefully designed and prepared set of complementary beam instrumentation and feedback systems. The design current of 400 mA was reached in April 2025, as expected without encountering CBM instabilities. First user pilot experiments were conducted in July 2025, where the operational FOFB improved the beam stability from 1-3000 Hz by a factor of four (X) and seven (Y), achieving an RMS stability of 144 nm (X) and 91 nm (Y), compared to a beam size in the order of ~10 µm. Further improvements and upgrades of SLS 1.0 systems temporarily taken over for SLS 2.0 are planned. The upgrade of insertion devices and beamlines has already started, but is still ongoing, using regular periodic shutdowns, as well as a 2nd shorter dark time in Q1/2026. This dark time will also be used to install newly designed super-bend magnets providing higher X-ray energies for their dipole beamlines.

ACKNOWLEDGEMENTS

The authors would like to thank all colleagues who contributed to the SLS 2.0 project.

REFERENCES

[1] A. Streun *et al.*, "SLS 2.0, the upgrade of the Swiss Light Source", in *Proc. IPAC'22*, Bangkok, Thailand, Jun. 2022, pp. 925-928. doi:10.18429/JACoW-IPAC2022-TUPOST032

[2] V. Schlott *et al.*, "The new SLS 2.0 booster-to-ring transfer line - design criteria, diagnostics layout and first beam results", presented at IBIC'25, Liverpool, UK, Sep. 2025, paper MOPMO19, this conference.

[3] M. Böge *et al.*, "SLS 2.0 storage ring commissioning", in *Proc. IPAC'25*, Taipei, Taiwan, Jun. 2025, paper WECN1, to be published. doi:10.18429/JACoW-IPAC2025-WECN1

[4] R. Ganter *et al.*, "SLS 2.0 storage ring upgrade overview", in *Proc. IPAC'25*, Taipei, Taiwan, Jun. 2025, paper MOPB005, to be published. doi:10.18429/JACoW-IPAC2025-MOPB005

[5] B. Keil *et al.*, "Development of the SLS 2.0 BPM system", in *Proc. IBIC'23*, Saskatoon, Canada, Sep. 2023, pp. 15-18. doi:10.18429/JACoW-IBIC2023-MO3C03

[6] C. Ozkan Loch *et al.*, "Diagnostic contributions to the commissioning of SLS 2.0", presented at IBIC'25, Liverpool, UK, Sep. 2025, paper MOPMO04, this conference.

[7] F. Armborst *et al.*, "Commissioning of the SLS 2.0 machine protection system", in *Proc. IPAC'25*, Taipei, Taiwan, Jun. 2025, paper TUPM057, to be published. doi:10.18429/JACoW-IPAC2025-TUPM057

[8] P. Baeta *et al.*, "First beam commissioning experience with RF system on chip based bunch by bunch signal processing systems at SLS 2.0", presented at IBIC'25, Liverpool, UK, Sep. 2025, paper MOPCO12, this conference.

[9] B. Keil *et al.*, "Directly Driving GHz-Range Power Amplifiers with RF Systems-On-Chip for the SLS 2.0 Longitudinal Multi-Bunch Feedback", in *Proc. IBIC'24*, Beijing, China, Sep. 2024. doi:10.18429/JACoW-IBIC2024-WEP42